Perifissural Nodules Seen at CT Screening for Lung Cancer[1]

Myeong I. Ahn, MD
Tadhg G. Gleeson, MD
Ida H. Chan, MD
Annette M. McWilliams, MBBS
Sharyn L. MacDonald, MD, MBChB
Stephen Lam, MD
Sukhinder Atkar-Khattra, BSc
John R. Mayo, MD

Purpose: To describe and characterize the potential for malignancy of noncalcified lung nodules adjacent to fissures that are often found in current or former heavy smokers who undergo computed tomography (CT) for lung cancer screening.

Materials and Methods: Institutional review board approval and informed consent were obtained. Baseline and follow-up thin-section multidetector CT scans obtained in 146 consecutive subjects at high risk for lung cancer (age range, 50–75 years; >30 pack-year smoking history) were retrospectively reviewed. Noncalcified nodules (NCNs) were categorized according to location (parenchymal, perifissural), shape, septal connection, manually measured diameter, diameter change, and lung cancer outcome at 7½ years.

Results: Retrospective review of images from 146 baseline and 311 follow-up CT examinations revealed 837 NCNs in 128 subjects. Of those 837 nodules, 234 (28%), in 98 subjects, were adjacent to a fissure and thus classified as perifissural nodules (PFNs). Multiple (range, 2–14) PFNs were seen in 47 subjects. Most PFNs were triangular (102/234, 44%) or oval (98/234, 42%), were located inferior to the carina (196/234, 84%), and had a septal connection (171/234, 73%). The mean maximal length was 3.2 mm (range, 1–13 mm). During 2-year follow-up in 71 subjects, seven of 159 PFNs increased in size on one scan but were then stable. The authors searched a lung cancer registry 7½ years after study entry and found 10 lung cancers in 139 of 146 study subjects who underwent complete follow-up; none of these cancers had originated from a PFN.

Conclusion: PFNs are frequently seen on screening CT scans obtained in high-risk subjects. Although PFNs may show increased size at follow-up CT, the authors in this study found none that had developed into lung cancer; this suggests that the malignancy potential of PFNs is low.

[1] From the Department of Radiology, Vancouver General Hospital, 899 W 12th Ave, Vancouver, BC, Canada V5Z 1M9 (M.I.A., T.G.G., I.H.C, S.L.M., J.R.M.); and the British Columbia Cancer Agency, Vancouver, BC, Canada (A.M., S.L., S.A.). Received January 21, 2009; revision requested February 25; revision received June 16; accepted July 16; final version accepted October 1. **Address correspondence to** J.R.M. (e-mail: *john.mayo@vch.ca*).

Lung cancer is now the most common cause of cancer-related death in both men and women. Because early lung cancer has minimal or nonspecific symptoms, most patients are found to have advanced disease at presentation (1,2). Although surgical, chemotherapy, and radiation therapy techniques (3,4) have progressed in the past 20 years, these advanced lesions remain resistant to therapy, and the overall 5-year survival rate, 15%, is unchanged. Multiple studies have shown that the best lung cancer survival occurs in the minority of patients who are found at presentation to have small early-stage lesions that are completely excised at surgery (3,5–7). Therefore, there is great interest in developing screening tests that help detect lung cancers as early as possible. Currently, the most promising technique for detecting early lung cancer in the lung parenchyma is nonenhanced computed tomography (CT).

Early lung cancer detection with CT is based on finding noncalcified nodules (NCNs) in the lung parenchyma that are thought to be the precursor to advanced lung cancers. Depending on the section thickness and nodule size criteria, nonrandomized lung cancer screening trials in high-risk current and former heavy smokers have revealed varying prevalences of NCNs, ranging from as low as 5.1% to as high as 51.4% (8). In these studies, the rate of surgically proved lung cancer has been shown to vary from 0.3% to 2.7% (7,9–14). Therefore, even in those subjects with the highest risk factors for lung cancer, most NCNs are benign.

Previous authors have studied benign and malignant NCNs to determine findings that enable confident classification. These study investigators have reported that polygonal shape, long-axis–to–short-axis diameter ratio (aspect ratio) greater than 1.78, peripheral location, lack of growth, and vascular attachment were the most suggestive findings of benign NCNs, some of which proved to be intrapulmonary lymph nodes (15–18). In reviewing contiguous thin-section nonenhanced CT images obtained with 1- or 1.25-mm collimation during the course of a nonrandomized single-arm lung cancer screening trial involving current or former heavy smokers, we noted a large number of NCNs that were adjacent to either major or minor fissures and showed the above benign characteristics. We named this subset of NCNs perifissural nodules (PFNs) and speculated that they might represent small lymph nodes and demonstrate benign behavior. Thus, the purpose of this investigation was to describe and characterize the malignancy potential of noncalcified lung nodules located adjacent to fissures that are often found in current or former heavy smokers who undergo CT to screen for lung cancer (19).

Advances in Knowledge

- Perifissural nodules (PFNs) are well-circumscribed, smoothly marginated nodules in contact with or closely related to a fissure.
- PFNs are most commonly triangular or oval, often show a septal attachment, and are usually located below the level of the carina.
- At 7½-year follow-up, no PFN had developed into a lung cancer; this led us to conclude that PFNs have a low likelihood of changing to malignancies.

Materials and Methods

Study Subjects

This study was approved by the University of British Columbia Clinical Ethics Review Board, and informed consent was obtained from all subjects. Between September and December 2001, as part of the Lung Health Study Protocol (19), 85 men and 61 women (mean age ± standard deviation, 59.9 years ± 6.9 and 57.9 years ± 6.3, respectively; P = .076) with a smoking history of more than 30 pack-years consecutively underwent low-radiation-dose chest CT to screen for lung cancer. Subjects with at least one NCN of any size were followed up with repeat regular-dose CT at 3–12-month intervals. The follow-up interval for the repeat CT scans was based on the maximal length of the largest nodule identified.

CT Technique and Follow-up Interval

Initial screening low-dose CT scans were obtained from the lung apex to the base by using an eight-channel multidetector CT scanner (LightSpeed Ultra QXi; GE Medical Systems, Milwaukee, Wis) at the following settings: 120 kVp, 80 mA, 0.5-second rotation time, 1.25-mm collimation, pitch of 1.35, volume CT dose index of 3.0 mGy, and effective section thickness (full width at half maximum, 3.87 mm) reconstructed at 1.25-mm intervals by using bone and standard algorithms. Until February 18, 2003, subjects harboring at least one NCN underwent follow-up regular-dose chest CT by using this eight-channel scanner at identical parameters, with the exception that the tube current was

Implication for Patient Care

- Up to one-third of all noncalcified lung nodules identified on nonenhanced screening chest CT scans obtained in current or former heavy smokers can be characterized as PFNs, which in this series were shown to have a low likelihood of being malignant, indicating the potential to avoid unnecessary follow-up or invasive investigations.

Published online
10.1148/radiol.09090031

Radiology 2010; 254:949–956

Abbreviations:
NCN = noncalcified nodule
PFN = perifissural nodule

Author contributions:
Guarantors of integrity of entire study, M.I.A., T.G.G., S.L., J.R.M.; study concepts/study design or data acquisition or data analysis/interpretation, all authors; manuscript drafting or manuscript revision for important intellectual content, all authors; manuscript final version approval, all authors; literature research, M.I.A., S.L., J.R.M.; clinical studies, all authors; statistical analysis, M.I.A., I.H.C., S.L., J.R.M.; and manuscript editing, M.I.A., T.G.G., S.L.M., S.L., J.R.M.

Authors stated no financial relationship to disclose.

increased to 320 mA and the volume CT dose index was increased to 12.0 mGy. After February 18, 2003, follow-up examinations were performed by using 16–detector row CT (Sensation 16; Siemens Medical Solutions, Forchheim, Germany) at the following settings: 120 kVp, 200 mA, 0.5-second rotation time, 1-mm collimation, pitch of 1.25, volume CT dose index of 9.73 mGy, and effective section thickness (full width at half maximum, 0.9 mm) reconstructed at 1-mm intervals by using B60 and B35 algorithm kernels. Note that follow-up images were obtained in these subjects, who had at least one NCN, at the regular radiation dose used at that time in our institution. We transitioned to a low dose (80 mA; volume CT dose index, 3.12 mGy) for all follow-up examinations in this lung cancer screening trial in December 2006.

The interval between follow-up CT examinations was determined according to the maximal length of the largest NCN. Follow-up was performed at 6, 12, and 24 months for small NCNs (range, 1–4 mm) and at 3, 6, 12, and 24 months for larger NCNs (range, 5–9 mm). The consulting respiratory physician and the subject jointly decided on the management of nodules larger than 10 mm by using follow-up CT scanning, needle biopsy, or surgical excision results.

Prospective Image Analysis

Baseline examination.—Per the Lung Health Study Protocol, all CT scans were prospectively reviewed for lung and mediastinal abnormalities by one of two subspecialty trained chest radiologists (S.M., J.R.M., 2 and 4 years of CT lung cancer screening experience, respectively). The number of cases reviewed by each observer was not recorded. One-millimeter or 1.25-mm contiguous transverse images were viewed by using lung (window width, 1500 HU; window level, −750 HU) and mediastinal (window width, 450 HU; window level, 35 HU) display parameters at a picture archiving and communication system (PACS) workstation (Agfa Health Care, Toronto, Ontario, Canada). Coronal reformations were used by the observers, as required, to confidently differentiate NCNs from vessels, pleural plaques, and linear scars, but they were not used for NCN diameter measurements. All NCNs were identified and annotated by using arrows on the PACS. The following data were recorded for each NCN by using computer software (Paradox for Windows, version 7; FileMaker, Santa Clara, Calif): maximal length measured with electronic calipers at the PACS workstation, location (parenchymal, perifissural), attenuation (solid, semisolid, or ground-glass opacity), and lung segmental location. Ancillary findings on the CT scans—including emphysema, bronchial wall thickening, respiratory bronchiolitis, mediastinal lymphadenopathy (1-cm short-axis criteria), and asbestos-related pleural disease—were recorded as present or absent. When one reviewer was unsure of the image findings, a consensus interpretation was performed. Consensus reviews were infrequent and were not recorded.

Follow-up examination.—Subjects with at least one NCN at prospective review underwent follow-up examinations (Fig 1). One of two reviewers (S.M., J.R.M.) interpreted the follow-up CT scans in conjunction with the scans obtained previously in the subjects by using two-monitor picture archiving and communication system stations. The database entries for all previous examinations of each NCN were available at the time of the review. By using the annotated previous images and with reference to vessels and bronchi, the reviewers confirmed that the correct NCN seen on the current images was comparable to the previous image findings and ensured that diameter measurements were performed identically at follow-up examinations. The change in size of each NCN was categorized as increased, unchanged, or decreased by using a cutoff of 1 mm; this value was determined in this lung cancer screening trial on the basis of experience. NCN volumetric assessments were used infrequently—only when the reviewing radiologists were unsure of the size change category—by using visual assessment or diameter measurements. Volumetric measurements were performed at a workstation (MMPW; Siemens Medical Solutions) equipped with a lung analysis software package (Syngo Lungcare, version Somaris/5 VB 10A; Siemens Medical Solutions). Volumetric measurements were not recorded. When one reviewer was unsure of the nodule growth classification, a

Figure 1

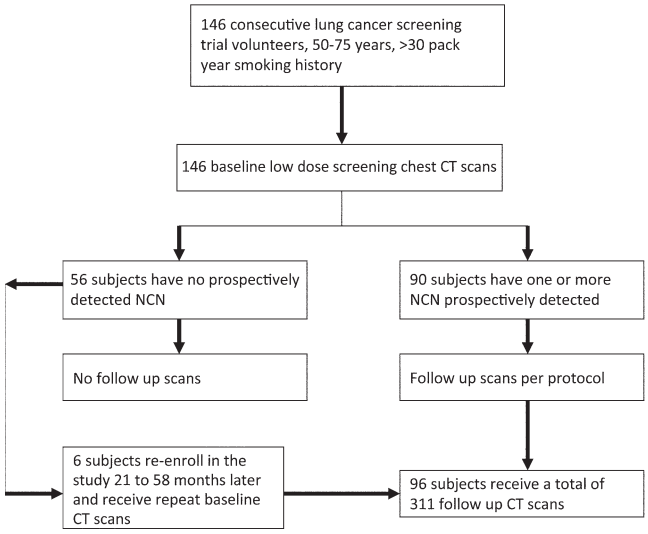

Figure 1: Flow diagram outline of CT examinations performed in 146 study subjects.

consensus review was performed. Consensus reviews were infrequent and not recorded.

Retrospective Nodule Analysis

From this ongoing lung cancer screening trial, a cohort of 146 consecutive patients who underwent CT between September 29, 2001, and December 9, 2001, was selected. Study CT scans were retrospectively re-evaluated in date order (Fig 2) by one radiologist (M.I.A.) with 1 year of CT lung cancer screening experience. She recorded in the database all detectable NCNs, with no minimal NCN size or maximal number criterion. Questionable NCNs were reviewed in consensus by two radiologists (M.I.A., J.R.M.). The number of consensus readings was not recorded. NCN was defined as any nonvascular, noncalcified soft-tissue mass of solid attenuation, semisolid attenuation, or ground-glass opacity that was visible at lung parenchymal window settings and noncalcified at mediastinal viewing settings. PFNs were a subset of NCNs that were solid, well circumscribed, smoothly marginated, and either in contact with or within 5 mm of a major, minor, or accessory fissure. Clustered PFN was defined as multiple PFNs within 10 mm of a fissure.

PFNs were counted, and the number of PFNs was compared with the total number of NCNs for all subjects. The long-axis and perpendicular short-axis diameters of each PFN were measured (M.I.A.) at the picture archiving and communication system workstation without magnification, and the aspect ratio (long-axis diameter/perpendicular diameter) was calculated (Table 1). PFN shape was classified as triangular, oval, round, rectangular, or dumbbell shaped (Fig 3) by using the transverse images. The relationships between shape, septal connection, and size were tabulated (Table 2). The location of the PFN relative to the fissure, carina, and segment was recorded (Table 3). Ancillary findings (emphysema, bronchial wall thickening, respiratory bronchiolitis, mediastinal lymphadenopathy [1-cm short-axis criteria], asbestos-related pleural disease) were recorded for later comparison with the presence of PFN.

Figure 2

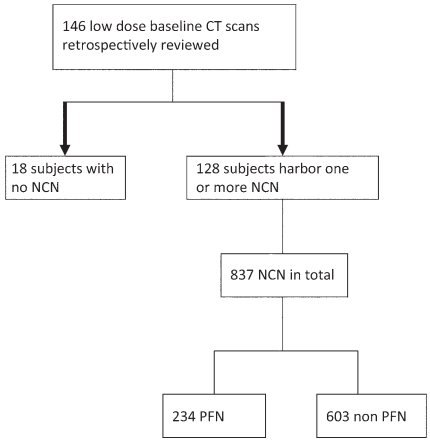

Figure 2: Flow diagram of the results of retrospective review of 146 low-radiation-dose baseline CT scans.

The follow-up scans of the 71 subjects who had undergone 24-month follow-up examination by October 13, 2004, were retrospectively reviewed by using the comparison technique previously described for the prospective review. Assessment of NCN growth was similar, again involving the use of a 1-mm threshold criterion on transverse images.

Long-term Follow-up

In April 2009, 7½ years after baseline CT scanning, longitudinal follow-up of all 146 subjects was performed. The subjects' names and birth dates were cross-referenced to the Cancer Registry of British Columbia, a continuously updated pathology database. By law, the pathology laboratories in the province of British Columbia are required to report all newly diagnosed cancers to this Registry. All (baseline and follow-up) CT scans obtained in subjects with diagnosed lung cancer were reviewed to determine if the cancer had originated from a previously identified PFN. The Lung Health Study database was reviewed to identify subjects who were lost to follow-up before the defined study endpoint, 24-month stability of all NCNs. In addition, the provincial Medical Services Plan demographics database was searched to identify those subjects who had left the province or were deceased.

Table 1

Size and Shape of PFNs

PFN Characteristic	No. of PFNs ($n = 234$)
Long-axis diameter (mm)	
1–4	187 (80)
5–9	44 (19)
≥10	3 (1)
Shape	
Triangular	102 (44)
Oval*	98 (42)
Round	18 (8)
Rectangular	13 (6)
Dumbbell shaped	3 (1)

Note.—Numbers in parentheses are percentages. The mean diameter of the PFNs was 3.2 mm ± 1.8 (standard deviation) (range, 1–13 mm). The mean ratio (long-axis diameter/perpendicular diameter) was 2.0 ± 1.8 (range, 1.0–3.5).

* Oval shape includes ovoid, lentiform, and half-moon shapes.

Statistical Analysis

Statistical analysis was performed by using computer software (SPSS for Windows V17.0; SPSS, Chicago, Ill). The χ^2 test of independence was used to assess the relationships between PFN and the following entities: emphysema, bronchial wall thickening, respiratory bronchiolitis, mediastinal lymphadenopathy, and asbestos-related pleural disease. $P < .05$ indicated significance.

Results

A total of 457 chest CT scans—146 screening images obtained at a low radiation dose and 311 follow-up images obtained at a regular dose—were reviewed. At retrospective review, 128 of 146 subjects (88%) had one (21/128, 16%) or more than one (107/128, 84%) NCN identified at the baseline screening examination (Fig 2). Significantly more subjects were found to have one or more NCNs at retrospective review (128/146) than at prospective review (90/146) ($P < .001$). At retrospective review, 837 NCNs were found in these 128 subjects, with an average

Figure 3

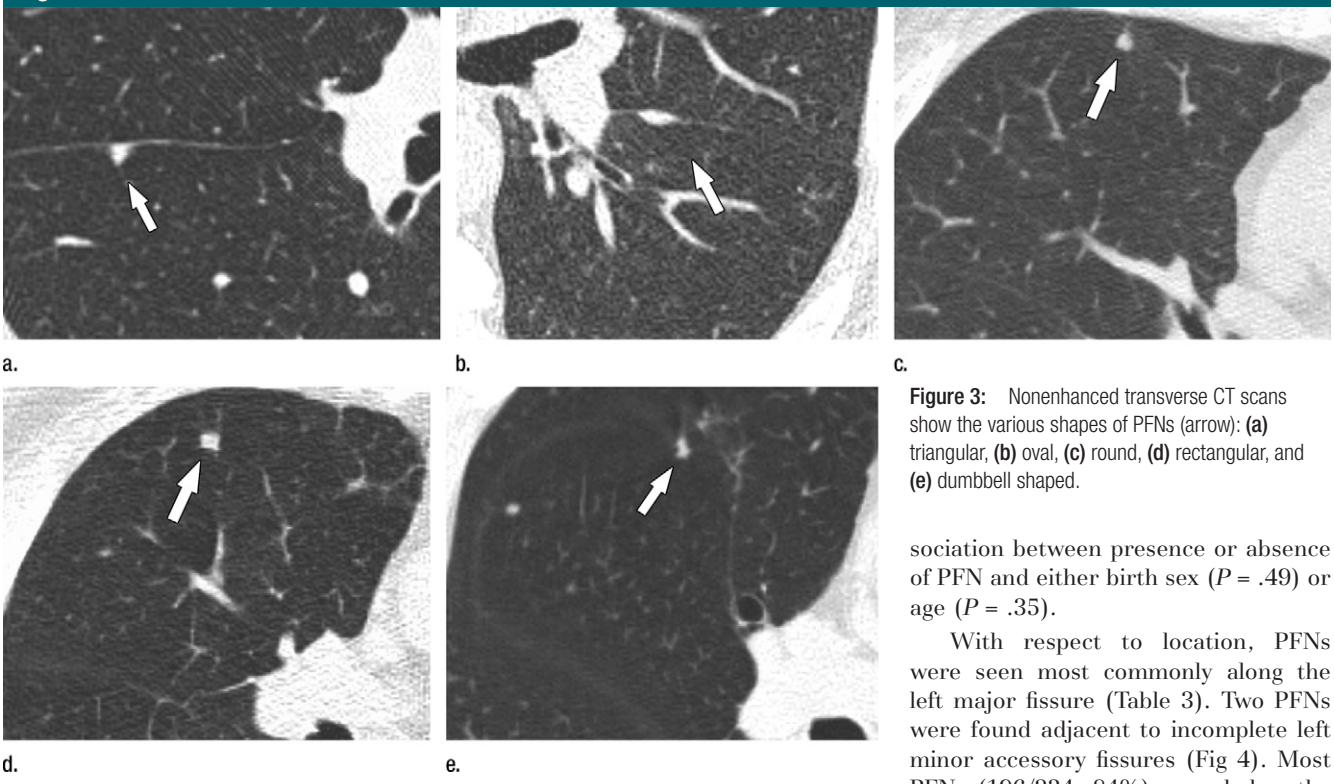

Figure 3: Nonenhanced transverse CT scans show the various shapes of PFNs (arrow): **(a)** triangular, **(b)** oval, **(c)** round, **(d)** rectangular, and **(e)** dumbbell shaped.

Table 2

Shape, Septal Connection, and Size of PFNs

Shape	Septal Connection*		Long-Axis Diameter (mm)†	Perpendicular Diameter (mm)†	Aspect Ratio‡
	Yes	No			
All (n = 234)	171 (73)	63 (27)	3.2	1.6	2.0
Triangular (n = 102)	86 (84)	16 (16)	2.9	1.5	1.9
Ovoid (n = 98)§	63 (64)	35 (36)	3.7	1.9	1.9
Round (n = 18)	7 (39)	11 (61)	1.2	1.0	1.2
Rectangular (n = 13)	12 (92)	1 (8)	4.7	1.5	3.1
Dumbbell shaped (n = 3)	3 (100)	0	5.7	1.9	3.0

* Numbers in parentheses are percentages.

† Data are mean values.

‡ Aspect ratio was determined as follows: long-axis diameter/perpendicular diameter.

§ Ovoid shape includes lentiform and crescent shapes.

of 6.5 NCNs (range, 1–31) per subject. Twenty-eight percent (234/837) of these NCNs fulfilled the criteria for a PFN (Fig 3). At least one PFN was seen in 98 of the 128 subjects (77%) with NCNs. Fifty-one of the 98 subjects (52%) had a single PFN, and 47 (48%) had multiple PFNs. Most PFNs were 1–4 mm in size (mean ± standard deviation, 3.2 mm ± 1.8) and triangular or oval (Table 1). The largest PFN was 13 × 8 mm. Eleven PFNs were clustered together (Fig 4). Seventy-three percent of PFNs (171/234) had a septal connection with the fissure (Table 2, Fig 5). With the exception of round PFNs, a septal connection was seen in more than half. There was no significant association between presence or absence of PFN and either birth sex (P = .49) or age (P = .35).

With respect to location, PFNs were seen most commonly along the left major fissure (Table 3). Two PFNs were found adjacent to incomplete left minor accessory fissures (Fig 4). Most PFNs (196/234, 84%) were below the level of the carina.

NCNs were detected in 90 subjects (Fig 1) at prospective review of baseline scans and in 128 subjects (Fig 2) at retrospective review. Therefore, 38 subjects with NCNs detected retrospectively did not undergo follow-up examinations. Six of these 38 subjects re-enrolled in a new phase of the institution's lung cancer screening program at 21–58 months (Fig 1). Thus, follow-up images were obtained in 96 of the 146 (66%) subjects. In these 96 subjects, the mean number of follow-up scans was 4.6 ± 2.5 (range, 1–11), and the mean duration of follow-up was 33 months ± 17 (range, 6–88 months). In date order, a sample of 71 of 96 subjects who underwent follow-up examinations was taken. These 71 subjects had 182 PFNs that were longitudinally reviewed for growth. One hundred sixty-nine of these 182 PFNs (93%) did not change in size during follow-up. Thirteen PFNs in nine subjects changed in size during the follow-up period. Six decreased in size (mean size changes: long axis, −1.4 mm ± 0.5 [standard

deviation]; perpendicular axis, –0.4 mm ± 0.7), and seven increased in size (mean size changes: long axis, 1.1 mm ± 0.7; perpendicular axis, 1.1 mm ± 0.7). Of the enlarging PFNs, four showed increased size on just one follow-up scan and then remained stable (Fig 6). Another two PFNs initially enlarged but then decreased in size and stayed stable. One PFN initially decreased in size, showed enlargement to its previous size on the subsequent scan, and then was stable for the remaining 14-month follow-up period. Five stable PFNs in two subjects were surgically resected as part of a lobectomy for lung cancer. None of these nodules was found to be malignant. No transfissural growth was seen in any PFN.

There was no significant association between presence or absence of PFN and emphysema (P = .10), bronchial wall thickening (P = .92), respiratory bronchiolitis (P = .98), or asbestos-related pleural disease (P = .53). No enlarged mediastinal lymph nodes were identified.

In April 2009, the 146 subjects in this trial were cross-referenced to the Cancer Registry of British Columbia. Up to that time, 10 lung cancers (6.8%)—four adenocarcinomas, four squamous cell carcinomas, and two small cell carcinomas—had been diagnosed in this cohort. Eight of the 10 cancers were either stage I at lobar resection (n = 7) or carcinoma in situ at bronchoscopy (n = 1). Of the other two cancers, one was stage IIA adenocarcinoma at lobectomy and the other was a small cell carcinoma with metastatic disease. At retrospective review, none of the lung cancers was found to have originated from a PFN. The Lung Health Study database revealed that four subjects were lost to follow-up at 7, 10, 12, and 15 months after baseline imaging. One of the subjects who was lost to follow-up had moved from the province. Review of the provincial Medical Services Plan database revealed that three additional subjects had moved from the province. Therefore, complete follow-up was achieved in 139 (95%) of 146 subjects. Nine subjects had died at the time of long-term follow-up.

Table 3

Location of PFNs

PFN Location	No. of PFNs (n = 234)
Fissures	
Left major	111 (47)
Right major	74 (32)
Right minor	47 (20)
Left minor accessory	2 (1)
Level	
Above carina	23 (10)
At level of carina	15 (6)
Below carina	196 (84)
Lobes and segments	
Right upper lobe	27 (11)
Posterior segment	12 (5)
Anterior segment	15 (6)
Right middle lobe	42 (18)
Lateral segment	21 (9)
Medial segment	21 (9)
Right lower lobe	54 (23)
Superior segment	29 (12)
Medial basal segment	9 (4)
Anterior basal segment	16 (7)
Left upper lobe	46 (20)
Apicoposterior segment	11 (5)
Anterior segment	4 (2)
Lingular division	31 (13)
Superior segment	15 (6)
Inferior segment	16 (7)
Left lower lobe	65 (28)
Superior segment	53 (23)
Anteromedial basal segment	12 (5)

Note.—Numbers in parentheses are percentages.

Discussion

Retrospective review of thin-section nonenhanced chest CT scans obtained in a cohort at high risk for lung cancer (age range, 50–75 years; >30 pack-year smoking history) and evaluated with no minimal size criteria for NCN revealed that 88% (128/146) of the subjects harbored at least one NCN. This rate of NCN detection in a high-risk population is higher than that previously reported (11%–69%) (9–14,19,20) and is likely secondary to both the thin-section CT technique used and the high sensitivity of the retrospective review process. At 7½-year follow-up, 10 lung cancers (10 of 146, 6.8%) had been diagnosed in this cohort, representing a malignant NCN rate of 1% (10 of 837). Because NCNs are so common compared with lung cancer, the challenge at lung cancer screening is to develop criteria that facilitate the differentiation between benign and malignant nodules.

In agreement with these study findings, previous reports indicate that most NCNs are benign (11–20). Currently, the most reliable criteria for identifying benign nodules are resolution of the nodule, complete calcification, and lack of growth during 2 years of follow-up (14,15,17,18). Although lack of growth for more than 2 years has been questioned as a marker of a benign nodule (21), it remains a commonly accepted standard. In our study, only seven PFNs showed any increase in size; however, they went on to remain stable in size for 15–67 months of follow-up.

Figure 4

Figure 4: Transverse CT scan shows three PFNs (arrows) clustered together along the accessory fissure separating the medial and lateral segments of the right middle lung lobe (arrowhead).

Figure 5

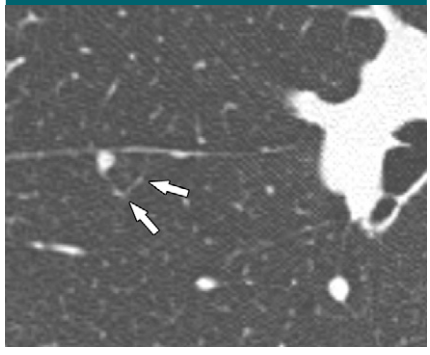

Figure 5: Transverse CT scan shows the septal connection (arrows) of a PFN.

Figure 6

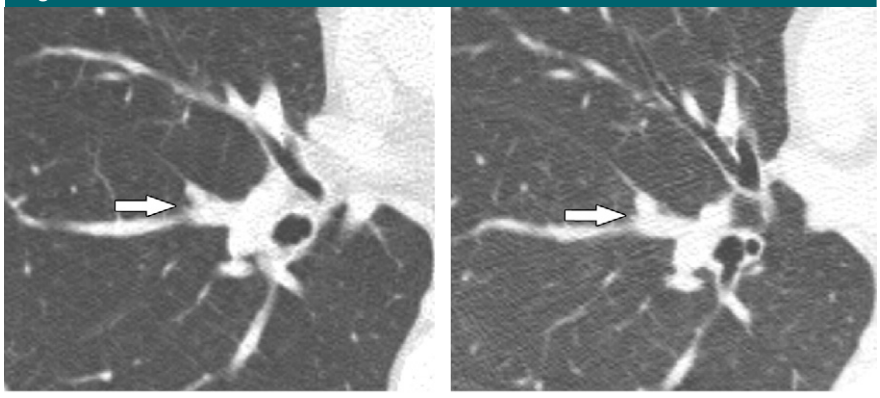

a. b.

Figure 6: Serial transverse CT scans show growth of a PFN during follow-up. **(a)** Baseline scan obtained at the level of the right middle lung lobe shows an ovoid PFN (arrow) abutting the medial portion of the right major fissure. **(b)** Scan obtained at 12-month follow-up shows that the PFN (arrow)—particularly its perpendicular diameter—increased in size. The PFN then remained stable for the following 15 months (not shown).

Figure 7

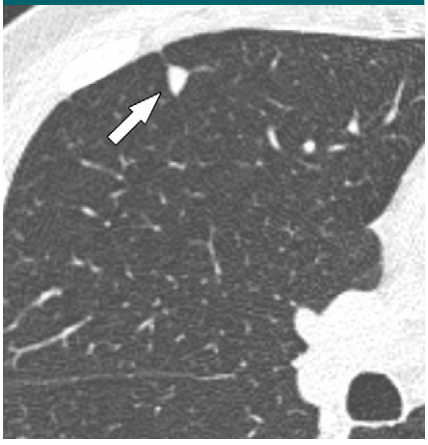

Figure 7: PFN confirmed to be an intrapulmonary lymph node at histopathologic examination. Transverse CT scan shows a triangular PFN (arrow) abutting the right minor fissure, with a septal connection. This PFN was removed by means of fuzzy-wire CT-guided video-assisted thoracoscopic wedge resection. An intrapulmonary lymph node was diagnosed at histopathologic examination.

We reviewed the provincial cancer registry data 7½ years after the start of the study to establish a longer-term follow-up. We found no evidence of a cancer originating from a PFN during this period. Although the total number of lung cancers in our cohort was 10, the failure to find a single cancer originating from a PFN suggests that the likelihood of a cancer arising from a PFN is low. An upper bound to the confidence interval surrounding the likelihood of a cancer originating from a PFN can be calculated on the basis of a sample size of 146 subjects (22). This upper-bound 95% confidence interval is calculated to be 2%. We can further extend these results by noting that we have not detected malignant transformation of a PFN during the past 9 years of this lung cancer screening trial. During this time, we examined 1828 subjects. By using this larger sample size, we can calculate an upper-bound 95% confidence interval of 0.16%.

Previous study investigators have identified NCN criteria for benignity (15,16); these criteria include predominantly solid, polygonal nodules in a subpleural location with a high aspect ratio. Published data from the NELSON trial (18) also indicated no cancers originating from smoothly marginated nodules or nodules attached to fissures, pleura, or adjacent vessels. We noted that most of the PFNs found in this study met these criteria.

These shape and location characteristics of PFNs suggest that they may represent intrapulmonary lymph nodes (23–28). Previous authors using surgical confirmation have noted that intrapulmonary lymph nodes are most frequently found in a subpleural location and inferior to the carina (23,24). Investigators in several studies have noted that intrapulmonary lymph nodes may abut or, via septa, be attached to the adjacent pleural surface (24,25,27). In one study (27), 10 (53%) of 19 intrapulmonary lymph nodes were adjacent to the visceral pleura, with the remaining nine located 2–8 mm from the pleura. Sykes et al (26) found that 70% of benign intrapulmonary lymph nodes showed a septal attachment. The finding that 73% of PFNs in this study showed a septal attachment represents circumstantial evidence that these nodules represent intraparenchymal lymph nodes. The septal lymphatic location may also explain the triangular or rectangular shape of approximately 50% of the PFNs in this study. Finally, we encountered a subject with an enlarging PFN (Fig 7) in our lung cancer screening trial that was not included in this study cohort. In this subject, the enlarging (7 × 8 mm) PFN was resected by using CT-guided fuzzy wire localization (29). This PFN was found to be a lymph node at histopathologic examination.

Three of 182 longitudinally followed up PFNs in this study showed both an increase and a decrease in size during CT follow-up. Trapnell (30) suggested that the inhalation of dust may cause transient hypertrophy of lymphoid tissue in the lung. Therefore, the change in size of a PFN may be secondary to a reaction to airborne stimuli. Enlarging intrapulmonary lymph nodes have also been previously reported in the literature (31,32). Finally, the identification of clusters of PFNs may be explained by the common activation of a group of intrapulmonary lymph nodes by an extrinsic stimulus.

Limitations of our study included the absence of histopathologic confirmation for the majority of the detected PFNs. We used two surrogate outcomes, 2-year stability and 7½-year follow-up of findings entered in the provincial cancer registry, as evidence of the nonmalignant nature of PFNs. We acknowledge that our electronic caliper manual measurements are less accurate and less reproducible for assessing the size of PFNs and determining their growth compared with computer-based volumetric analysis (33,34). However, given the large number of PFNs assessed, the small size of many of the PFNs (100 of 234 were <2 mm in maximal diameter), and the proximity to the

fissure leading to segmentation issues, we believed that automated volumetric analysis was not feasible in this study (35,36). Finally, use of our retrospective analysis technique led to a somewhat inflated number of identified NCNs and PFNs, as we have noted that many radiologists tend to either ignore or fail to identify these nodules at prospective review. In this study, this statement was supported by the finding at retrospective review of at least one NCN in 38 subjects who were classified as having no NCN at prospective review.

In conclusion, PFNs are frequently seen on screening CT images obtained in subjects at high risk of developing lung cancer, and although these nodules may show an increase in size at follow-up examinations, none showed progressive growth over multiple consecutive examinations or developed into lung cancer during 7½ years of follow-up in our investigation.

References

1. Manser RL, Irving LB, Stone C, Byrnes G, Abramson M, Campbell D. Screening for lung cancer. Cochrane Database Syst Rev 2001;3:CD001991.
2. Jemal A, Murray T, Samuels A, Ghafoor A, Ward E, Thun MJ. Cancer statistics, 2003. CA Cancer J Clin 2003;53:5–26.
3. Fry WA, Menck HR, Winchester DP. The National Cancer Data Base Report on Lung Cancer. Cancer 1996;77:1947–1955.
4. Cohen V, Khuri FR. Chemoprevention of lung cancer: current status and future prospects. Cancer Metastasis Rev 2002;21:349–362.
5. Martini N, Rusch VW, Bains MS, et al. Factors influencing ten-year survival in resected stages I to IIIa non-small cell lung cancer. J Thorac Cardiovasc Surg 1999;117:32–36.
6. Cortese DA, Pariolero PC, Bergstralh EJ, et al. Roentgenographically occult lung cancer: a ten-year experience. J Thorac Cardiovasc Surg 1983;86:373–380.
7. Henschke CI, McCauley DI, Yankelevitz DF, et al. Early Lung Cancer Action Project: overall design and findings from baseline screening. Lancet 1999;354:99–105.
8. Bepler G, Carney DG, Djulbegovic B, Clark RA, Tockman M. A systematic review and lessons learned from early lung cancer detection trials using low-dose computed tomography of the chest. Cancer Control 2003;10:306–314.
9. Kaneko M, Eguchi K, Ohmatsu H, et al. Peripheral lung cancer: screening and detection with low-dose spiral CT versus radiography. Radiology 1996;201:798–802.
10. Sobue T, Moriyama N, Kaneko M, et al. Screening for lung cancer with low-dose helical computed tomography: anti-lung cancer association project. J Clin Oncol 2002;20:911–920.
11. Henschke CI, Naidich DP, Yankelevitz DF, et al. Early Lung Cancer Action Project: initial findings on repeat screenings. Cancer 2001;92:153–159.
12. Sone S, Li F, Yang ZG, et al. Results of three-year mass screening programme for lung cancer using mobile low-dose spiral computed tomography scanner. Br J Cancer 2001;84:25–32.
13. Diederich S, Wormanns D, Semik M. Screening for early lung cancer with low-dose spiral CT: prevalence in 817 asymptomatic smokers. Radiology 2002;222:773–781.
14. Swensen SJ, Jett JR, Hartman TE, et al. Lung cancer screening with CT: Mayo Clinic experience. Radiology 2003;226:756–761.
15. Takashima S, Sone S, Li F, et al. Small solitary pulmonary nodules (≤1 cm) detected at population-based CT screening for lung cancer: reliable high-resolution CT features of benign lesions. AJR Am J Roentgenol 2003;180:955–964.
16. Takashima S, Sone S, Li F, Maruyama Y, Hasegawa M, Kadoya M. Indeterminate solitary pulmonary nodules revealed at population-based CT screening of the lung: using first follow-up diagnostic CT to differentiate benign and malignant lesions. AJR Am J Roentgenol 2003;180:1255–1263.
17. Benjamin MS, Drucker EA, McLoud TC, Shepard JA. Small pulmonary nodules: detection at chest CT and outcome. Radiology 2003;226:489–493.
18. Xu DM, van der Zaag-Loonen HJ, Oudkerk M, et al. Smooth or attached solid indeterminate nodules detected at baseline CT screening in the NELSON Study: cancer risk during 1 year follow-up. Radiology 2009; 250:264–272.
19. McWilliams A, Mayo JR, MacDonald S, et al. Lung cancer screening: a different paradigm. Am J Respir Crit Care Med 2003;168:1167–1173.
20. MacRedmond R, Logan PM, Lee M, Kenny D, Foley C, Costello RW. Screening for lung cancer using low dose CT scanning. Thorax 2004;59:237–241.
21. Yankelevitz DF, Henschke CI. Does 2-year stability imply that pulmonary nodules are benign? AJR Am J Roentgenol 1997; 168:325–328.
22. Hanley JA, Lippman-Hand A. If nothing goes wrong, is everything all right? interpreting zero numerators. JAMA 1983; 249:1743–1745.
23. Bankoff MS, McEniff NJ, Bhadelia RA, Garcia-Moliner M, Daly BD. Prevalence of pathologically proven intrapulmonary lymph nodes and their appearance on CT. AJR Am J Roentgenol 1996;167:629–630.
24. Yokomise H, Mizuno H, Ike O, Wada H, Hitomi S, Itoh H. Importance of intrapulmonary lymph nodes in the differential diagnosis of small pulmonary nodular shadows. Chest 1998;113:703–706.
25. Matsuki M, Noma S, Kuroda Y, Oida K, Shindo T, Kobashi Y. Thin-section CT features of intrapulmonary lymph nodes. J Comput Assist Tomogr 2001;25:753–756.
26. Sykes AM, Swensen SJ, Tazelaar HD, Jung SH. Computed tomography of benign intrapulmonary lymph nodes: retrospective comparison with sarcoma metastases. Mayo Clin Proc 2002;77:329–333.
27. Oshiro Y, Kusumoto M, Moriyama N, et al. Intrapulmonary lymph nodes: thin-section CT features of 19 nodules. J Comput Assist Tomogr 2002;26:553–557.
28. Kradin RL, Spirn PW, Mark EJ. Intrapulmonary lymph nodes: clinical, radiologic, and pathologic features. Chest 1985;87:662–667.
29. Mayo JR, Clifton JC, Powell TI, et al. Lung nodules: CT-guided placement of microcoils to direct video-assisted thoracoscopic surgical resection. Radiology 2009;250:576–585.
30. Trapnell DH. Recognition and incidence of intrapulmonary lymph nodes. Thorax 1964;19:44–50.
31. Houk VN, Osborne DP. Subvisceral pleural lymph node presenting as an expanding intrapulmonary nodule. Am Rev Respir Dis 1965;91:596–599.
32. Ehrenstein FI. Pulmonary lymph node presenting as an enlarging coin lesion. Am Rev Respir Dis 1970;101:595–599.
33. Yankelevitz DF, Gupta R, Zhao B, Henschke CI. Small pulmonary nodules: evaluation with repeat CT—preliminary experience. Radiology 1999;212:561–566.
34. Reeves AP, Chan AB, Yankelevitz DF, Henschke CI, Kressler B, Kostix WJ. On measuring the change in size of pulmonary nodules. IEEE Trans Med Imaging 2006;25:435–450.
35. Ravenel JG, Leue WM, Nietert PJ, Miller JV, Taylor KK, Silvestri GA. Pulmonary nodule volume: effects of reconstruction parameters on automated measurements—a phantom study. Radiology 2008;247:400–408.
36. Wang Y, van Klaveren RJ, van der Zaag-Loonen HJ, et al. Effect of nodule characteristics on variability of semiautomated volume measurements in pulmonary nodules detected in a lung cancer screening program. Radiology 2008;248:625–631.